

Article

Bioactivity-Guided Screening of Antimicrobial Secondary Metabolites from Antarctic Cultivable Fungus *Acrostalagmus luteoalbus* CH-6 Combined with Molecular Networking

Ting Shi ^{1,2} , Xiang-Qian Li ^{2,3} , Ze-Min Wang ², Li Zheng ^{4,5}, Yan-Yan Yu ², Jia-Jia Dai ² and Da-Yong Shi ^{2,3,*}

¹ College of Chemical and Biological Engineering, Shandong University of Science and Technology, Qingdao 266590, China; shiting_jia@126.com

² State Key Laboratory of Microbial Technology, Institute of Microbial Technology, Shandong University, Qingdao 266200, China; lixiangqian@sdu.edu.cn (X.-Q.L.); zemin3210@163.com (Z.-M.W.); yuyanyan@sdu.edu.cn (Y.-Y.Y.); daijiajia@sdu.edu.cn (J.-J.D.)

³ Laboratory for Marine Drugs and Bioproducts of Qingdao National Laboratory for Marine Science and Technology, Qingdao 266071, China

⁴ Key Laboratory of Marine Eco-Environmental Science and Technology, First Institute of Oceanography, Ministry of Natural Resources, Qingdao 266061, China; zhengli@fio.org.cn

⁵ Laboratory for Marine Ecology and Environmental Science, Qingdao Pilot National Laboratory for Marine Science and Technology, Qingdao 266071, China

* Correspondence: shidayong@sdu.edu.cn

Abstract: With the increasingly serious antimicrobial resistance, discovering novel antibiotics has grown impendently. The Antarctic abundant microbial resources, especially fungi, can produce unique bioactive compounds for adapting to the hostile environment. In this study, three Antarctic fungi, *Chrysosporium* sp. HXSXD-11-1, *Cladosporium* sp. HXSXD-12 and *Acrostalagmus luteoalbus* CH-6, were found to have the potential to produce antimicrobial compounds. Furthermore, the crude extracts of CH-6 displayed the strongest antimicrobial activities with 72.3–84.8% growth inhibition against *C. albicans* and *Aeromonas salmonicida*. The secondary metabolites of CH-6 were researched by bioactivity tracking combined with molecular networking and led to the isolation of two new α -pyrones, acrostalapyrones A (1) and B (2), along with one known analog (3), and three known indole diketopiperazines (4–6). The absolute configurations of 1 and 2 were identified through modified Mosher's method. Compounds 4 and 6 showed strong antimicrobial activities. Remarkably, the antibacterial activity of 6 against *A. salmonicida* displayed two times higher than that of the positive drug Ciprofloxacin. This is the first report to discover α -pyrones from the genus *Acrostalagmus*, and the significant antimicrobial activities of 4 and 6 against *C. albicans* and *A. salmonicida*. This study further demonstrates the great potential of Antarctic fungi in the development of new compounds and antibiotics.

Keywords: Antarctic fungi; bioactivity-guided screening; molecular networking; antimicrobial activities; secondary metabolites; *Acrostalagmus luteoalbus*; indole diketopiperazines; α -pyrones



Citation: Shi, T.; Li, X.-Q.; Wang, Z.-M.; Zheng, L.; Yu, Y.-Y.; Dai, J.-J.; Shi, D.-Y. Bioactivity-Guided Screening of Antimicrobial Secondary Metabolites from Antarctic Cultivable Fungus *Acrostalagmus luteoalbus* CH-6 Combined with Molecular Networking. *Mar. Drugs* **2022**, *20*, 334. <https://doi.org/10.3390/md20050334>

Academic Editor: Andrew P. Desbois

Received: 20 April 2022

Accepted: 17 May 2022

Published: 19 May 2022

Publisher's Note: MDPI stays neutral with regard to jurisdictional claims in published maps and institutional affiliations.



Copyright: © 2022 by the authors. Licensee MDPI, Basel, Switzerland. This article is an open access article distributed under the terms and conditions of the Creative Commons Attribution (CC BY) license (<https://creativecommons.org/licenses/by/4.0/>).

1. Introduction

Antimicrobial drugs, including antibiotics, antivirals, antifungals, and antimalarials, are medicines that are active against various infections [1]. However, antimicrobial resistance (AMR) has become an increasing state when microorganisms develop resistance to antimicrobial drugs, leading to invalid treatment with existing drugs [2]. AMR is a global concern as new resistance mechanisms are emerging and spreading globally, threatening our ability to treat common infectious diseases, and resulting in prolonged illness, disability, and death [3]. In 2019, WHO declared AMR as one of the top 10 global public health threats facing humanity [4]. Each year in the U.S., at least 2.8 million people are infected with antibiotic-resistant bacteria or fungi, and more than 35,000 people die as a result [5]. In

Europe, antibiotic resistance is responsible for an estimated 33,000 deaths annually [6]. In this stage, it is an urgent requirement to discover novel effective antibiotics to respond to the challenge of antibiotic-resistant bacteria or fungi. Natural products from microorganisms have played a significant role in delivering antibiotics since the discovery of penicillin in the 1940s [7]. New microbial species in special environments and new approaches such as genome mining and high throughput chemical screening are required to exploit novel antibiotics to answer the challenge of AMR [8].

The harsh environment of Antarctica, including cold, dry and intense ultraviolet irradiation, gives the microbes unique physiological and biochemical characteristics and possesses the capacity to produce novel bioactivities and secondary metabolites [9]. In recent years, many new compounds with antibacterial or antifungal activities have been found in Antarctic fungi. For example, new polyketides ketidocillinones B and C, isolated from Antarctic sponge-derived fungus, exhibited potent antibacterial activities against *Pseudomonas aeruginosa*, *Mycobacterium phlei*, and MRCNS (methicillin-resistant coagulase-negative staphylococci) [10]. For another example, new aspochracin-type cyclic tripeptides sclerotiotides M and N, deriving from Antarctic fungus, showed broad antimicrobial activities against a panel of pathogenic strains [11]. Our recent findings also discovered a new polyketide pseudophenone A, produced by an Antarctic fungus, exhibited antibacterial activities against a panel of strains [12].

To find novel antibiotics, culturable fungi from soil samples, collected from Fildes Peninsula, Antarctica, were isolated and purified, and it was found that three of the fungi crude extracts, *Chrysosporium* sp. HSXSD-11-1, *Cladosporium* sp. HSXSD-12 and *Acrostalagmus luteoalbus* CH-6, exhibited significant antifungal activities and the crude extracts of *A. luteoalbus* CH-6 showed the strongest antifungal and antibacterial activities. A series of active compounds, focusing on alkaloids and terpenoids, had been isolated from the genus of *Acrostalagmus* by previous researchers [13–22], which further proved the potential capacity of the fungus *A. luteoalbus* CH-6 to produce novel antibiotics. Molecular networking has become an outstanding method to visualize and identify the secondary metabolites of the fungi crude extracts in non-targeted MS² data [23–25]. Hence, we performed systematic research on secondary metabolites of the fungus *A. luteoalbus* CH-6 with the strategies of bioactivity tracking and molecular networking. In this report, the bioactivity screening of the antimicrobial fungi, and the isolation, structure elucidation, and antimicrobial activity evaluations of the isolated compounds are reported and discussed.

2. Results and Discussion

2.1. Isolation and Antimicrobial Screening of Soil-Derived Fungi from Fildes Peninsula, Antarctica

Eighty-two strains of cultivable fungi were isolated from the soil samples, collected in Fildes Peninsula, Antarctica, at the Chinese 35th Antarctic expedition in 2019. According to their different community morphology (Figure S1), 26 strains were selected and fermented by two culture conditions to obtain 52 crude extracts. The antimicrobial activities of the 52 crude extracts were evaluated by one pathomycete, four pathogenic bacteria, and ten marine fouling bacteria (Tables 1–3). Three fungal crude extracts, numbered HSXSD-11-1, HSXSD-12, and CH-6, exhibited significant antifungal activity against *C. albicans* with 71.4–78.7% growth inhibition at 50 µg/mL (Table 1). Among them, the strain CH-6 displayed the strongest antimicrobial activities against *C. albicans* and *A. salmonicida* with 72.3–84.8% growth inhibition (Tables 1 and 2).

Table 1. Antimicrobial activities of the culture filtrate extracts (50 µg/mL) of the Antarctic-soil-derived fungi against one pathomycete and four pathogenic bacteria.

Strain Number	Inhibition Rate % ^a (Staticity/Shaking)				
	<i>C. albicans</i>	<i>E. coli</i>	<i>S. aureus</i>	<i>B. subtilis</i>	<i>P. aeruginosa</i>
HSXSD-11-1	75.0 ± 3.9/71.4 ± 0.7	-/15.2 ± 4.2	41.4 ± 2.6/40.3 ± 1.8	13.6 ± 0.5/18.0 ± 4.6	-/-
HSXSD-12	76.0 ± 3.1/-	-/-	-/25.1 ± 0.6	-/12.9 ± 2.8	-/-
HSX2#-13	-/-	-/-	-/-	-/16.6 ± 2.5	-/-
HSX6#-16	-/18.9 ± 4.1	-/-	-/24.0 ± 1.5	15.7 ± 4.8/21.4 ± 1.0	10.4 ± 2.4/11.9 ± 4.2
CH-6	78.7 ± 1.2/72.3 ± 0.8	-/-	39.3 ± 3.7/49.6 ± 4.1	19.2 ± 2.4/17.8 ± 0.3	12.8 ± 4.0/16.1 ± 4.6
CH-9	-/-	-/-	-/-	12.2 ± 2.1/17.1 ± 0.5	-/-
DLW-10	-/12.2 ± 4.9	17.1 ± 1.3/17.6 ± 3.0	20.6 ± 4.5/24.4 ± 1.1	-/12.3 ± 2.8	-/-
WLG-10	-/-	21.5 ± 2.7/-	16.9 ± 2.3/-	-/-	-/-
HSXSD-6	-/-	-/14.1 ± 2.4	-/-	-/12.8 ± 3.2	-/-
HSXSD-10	-/-	13.8 ± 1.0/16.6 ± 1.9	-/22.5 ± 0.1	-/15.3 ± 0.8	-/-
HSX2#-5	-/-	22.2 ± 2.4/-	-/16.4 ± 0.7	-/18.7 ± 1.3	-/12.3 ± 2.8
HSX2#-7	-/-	10.2 ± 2.6/-	-/13.8 ± 1.5	-/14.4 ± 1.7	-/17.1 ± 2.0
HSX2#-11	29.6 ± 4.5/14.3 ± 3.6	-/-	19.6 ± 3.5/27.3 ± 0.2	12.9 ± 1.3/18.2 ± 1.2	-/-
HSX2#-12	23.2 ± 2.4/22.7 ± 1.8	-/-	18.6 ± 0.5/27.9 ± 0.1	14.7 ± 5.1/-	-/-
HSX2#-15	21.7 ± 6.8/-	-/-	-/12.8 ± 2.1	15.1 ± 4.5/11.5 ± 0.7	-/-
HSX11#-3	24.7 ± 4.9/-	-/12.6 ± 9.5	-/22.1 ± 0.8	16.1 ± 2.5/-	-/-
HSX11#-4	20.5 ± 3.2/-	-/-	-/-	12.8 ± 0.5/15.2 ± 1.6	-/-
HSX6#-8	-/-	11.7 ± 4.0/14.4 ± 0.8	-/26.4 ± 2.6	10.2 ± 1.1/-	-/-
HSX6#-10	30.3 ± 2.0/-	23.1 ± 2.2/-	20.8 ± 1.4/25.5 ± 0.0	17.0 ± 3.5/15.3 ± 0.9	-/-
HSX6#-14	16.1 ± 5.4/-	11.1 ± 2.8/16.0 ± 2.9	24.4 ± 5.0/-	-/-	-/-
HSX8#-6	20.6 ± 1.4/-	-/13.7 ± 0.1	22.2 ± 2.7/10.9 ± 8.8	16.3 ± 1.9/-	-/-
HSX8#-9	15.9 ± 2.5/-	11.1 ± 3.8/-	21.9 ± 0.1/-	-/-	-/-
JQW-6	24.4 ± 4.7/-	11.0 ± 1.1/-	-/-	19.4 ± 2.5/-	-/-
JQW-8	18.3 ± 4.4/-	-/-	10.5 ± 1.0/-	21.3 ± 2.3/12.7 ± 3.2	-/-
WLG-7	11.1 ± 1.4/-	-/-	-/-	11.3 ± 2.2/-	-/-
DLW-7	-/-	-/-	-/-	-/-	-/-
CH-6-rice	80.5 ± 0.9	-	48.2 ± 2.5	19.8 ± 1.6	18.1 ± 3.1
CPFEX (10 µM)	66.2 ± 1.8	76.5 ± 2.3	79.1 ± 1.1	81.9 ± 3.4	70.2 ± 3.3

^a The inhibition rate: >60% was intense, 40–60% was media, 20–40% is low, and <20% was no activity, <10% was not shown.

Table 2. Antimicrobial activities of the culture filtrate extracts (50 µg/mL) of the Antarctic-soil-derived fungi against five marine fouling bacteria.

Strain Number	Inhibition Rate % ^a (Staticity/Shaking)				
	<i>A. salmonicida</i>	<i>V. anguillarum</i>	<i>P. angustum</i>	<i>P. aeruginosa</i>	<i>P. halotolerans</i>
HSXSD-11-1	-/-	26.4 ± 2.6/32.0 ± 1.5	16.8 ± 2.3/14.6 ± 1.0	18.4 ± 4.5/14.9 ± 3.7	-/-
HSXSD-12	-/-	29.6 ± 3.5/-	16.1 ± 1.3/10.1 ± 2.0	12.1 ± 0.6/-	-/-
HSX2#-13	-/-	-/11.4 ± 2.9	16.8 ± 1.6/-	10.7 ± 0.6/-	-/-
HSX6#-16	-/-	24.5 ± 3.6/24.4 ± 0.5	17.5 ± 0.7/14.5 ± 1.1	-/-	-/-
CH-6	84.8 ± 1.4/77.6 ± 1.0	50.6 ± 2.6/58.3 ± 3.1	12.9 ± 0.8/14.4 ± 0.4	22.1 ± 2.5/13.4 ± 4.0	-/-
CH-9	-/-	10.9 ± 2.2/10.2 ± 0.2	13.2 ± 0.3/11.8 ± 0.8	-/-	-/-
DLW-10	-/-	-/20.8 ± 2.9	-/-	-/-	-/-
WLG-10	-/-	-/-	10.8 ± 0.5/-	16.8 ± 0.1/-	-/-
HSXSD-6	-/-	-/-	13.1 ± 1.7/-	-/-	-/-
HSXSD-10	-/-	-/-	-/-	-/-	-/-
HSX2#-5	-/-	-/-	-/-	-/-	-/-
HSX2#-7	-/-	-/-	12.3 ± 0.8/-	-/-	-/-
HSX2#-11	33.4 ± 2.5/13.3 ± 4.1	-/-	13.7 ± 1.2/-	-/-	-/-
HSX2#-12	-/17.4 ± 3.8	18.3 ± 0.8/-	13.7 ± 1.0/-	-/-	-/-
HSX2#-15	-/13.9 ± 3.8	19.2 ± 0.7/-	14.0 ± 0.1/-	-/-	-/-
HSX11#-3	-/-	23.8 ± 0.6/-	10.6 ± 1.0/-	-/-	-/-
HSX11#-4	-/17.9 ± 0.7	-/-	-/-	-/-	-/-
HSX6#-8	-/-	-/-	-/-	-/-	-/-
HSX6#-10	-/-	12.7 ± 1.5/-	-/-	-/-	-/-
HSX6#-14	-/-	-/-	-/14.3 ± 2.9	-/-	-/-
HSX8#-6	-/22.3 ± 4.5	-/-	-/14.5 ± 5.2	-/-	-/-
HSX8#-9	-/-	-/-	-/16.7 ± 3.0	-/-	-/-

Table 2. Cont.

Strain Number	Inhibition Rate % ^a (Staticity/Shaking)				
	<i>A. salmonicida</i>	<i>V. anguillarum</i>	<i>P. angustum</i>	<i>P. aeruginosa</i>	<i>P. halotolerans</i>
JQW-6	13.6 ± 2.4/-	21.5 ± 3.2/-	-/16.7 ± 2.4	-/-	-/-
JQW-8	14.6 ± 2.4/-	18.2 ± 0.6/-	10.6 ± 1.5/13.3 ± 0.8	-/-	-/-
WLG-7	21.8 ± 2.1/-	12.8 ± 4.1/-	10.2 ± 0.5/12.4 ± 2.7	-/-	-/-
DLW-7	-/-	-/-	-/11.7 ± 0.9	-/-	-/-
CH-6-rice	86.7 ± 1.1	57.1 ± 2.4	12.2 ± 3.2	20.9 ± 3.1	-
Sea-nine 211 (10 µM)	78.1 ± 3.7	71.0 ± 2.1	81.5 ± 2.9	69.1 ± 2.1	67.5 ± 4.5

^a The inhibition rate: >60% was intense, 40–60% was media, 20–40% is low, and <20% was no activity, <10% was not shown.

Table 3. Antimicrobial activities of the culture filtrate extracts (50 µg/mL) of the Antarctic-soil-derived fungi against another five marine fouling bacteria.

Scheme Number	Inhibition Rate % ^a (Staticity/Shaking)				
	<i>E. cloacae</i>	<i>E. hormaechei</i>	<i>P. fulva</i>	<i>V. harveyi</i>	<i>A. hydrophila</i>
HSXSD-11-1	-/-	12.0 ± 1.9/-	-/-	15.5 ± 1.8/12.6 ± 1.3	-/-
HSXSD-12	-/-	-/-	10.1 ± 2.2/-	16.2 ± 3.6/10.3 ± 2.9	-/-
HSX2#-13	10.5 ± 0.7/19.1 ± 0.7	10.3 ± 0.3/12.9 ± 0.5	-/12.8 ± 0.8	16.9 ± 3.2/11.7 ± 3.9	-/12.8 ± 0.7
HSX6#-16	13.3 ± 1.6/14.0 ± 1.8	11.6 ± 1.0/-	14.3 ± 1.8/10.4 ± 0.8	18.6 ± 1.6/10.5 ± 2.3	-/-
CH-6	-/-	10.1 ± 0.6/15.4 ± 0.8	11.4 ± 2.2/13.3 ± 1.2	20.0 ± 0.6/21.0 ± 0.9	19.4 ± 3.5/14.3 ± 2.3
CH-9	21.1 ± 3.2/21.0 ± 0.4	11.5 ± 2.3/14.1 ± 0.3	12.2 ± 3.2/18.8 ± 1.1	13.1 ± 3.5/15.5 ± 1.9	-/13.5 ± 1.6
DLW-10	-/-	-/-	-/11.9 ± 2.2	13.9 ± 1.8/15.5 ± 2.1	-/-
WLG-10	-/-	-/-	-/-	-/-	-/-
HSXSD-6	13.1 ± 7.5/-	-/-	-/-	13.4 ± 1.5/10.7 ± 0.7	-/-
HSXSD-10	-/-	-/-	-/-	-/11.2 ± 1.7	-/-
HSX2#-5	-/10.1 ± 1.0	-/-	-/-	-/10.1 ± 1.2	-/-
HSX2#-7	-/-	-/-	-/-	-/10.8 ± 1.8	-/-
HSX2#-11	-/-	-/-	-/-	10.8 ± 3.2/-	-/-
HSX2#-12	-/-	-/-	-/-	12.4 ± 2.9/13.3 ± 1.7	-/-
HSX2#-15	10.3 ± 4.2/-	-/-	-/-	15.3 ± 1.4/13.3 ± 1.5	-/-
HSX11#-3	15.3 ± 0.5/-	-/-	-/-	15.2 ± 1.4/-	-/-
HSX11#-4	19.0 ± 0.6/-	10.7 ± 0.6/-	10.2 ± 2.6/-	12.6 ± 1.3/11.0 ± 2.9	11.9 ± 1.1/-
HSX6#-8	-/-	-/-	-/-	-/-	-/-
HSX6#-10	-/-	-/-	-/-	-/11.2 ± 2.8	-/-
HSX6#-14	-/-	-/11.1 ± 0.7	-/-	-/-	-/-
HSX8#-6	-/-	-/-	-/-	-/13.2 ± 2.8	-/-
HSX8#-9	-/-	-/11.3 ± 1.2	-/10.6 ± 1.9	-/14.4 ± 4.3	-/-
JQW-6	13.7 ± 0.8/-	-/11.9 ± 0.4	-/10.1 ± 1.1	-/16.0 ± 4.0	-/-
JQW-8	19.1 ± 1.0/-	10.2 ± 0.7/10.5 ± 1.2	-/-	15.0 ± 1.4/15.9 ± 1.2	11.5 ± 0.5/-
WLG-7	19.8 ± 0.7/-	-/-	-/-	15.1 ± 1.8/13.7 ± 3.7	12.0 ± 0.4/-
DLW-7	-/15.2 ± 2.9	-/-	-/-	-/14.5 ± 2.5	-/-
CH-6-rice	-	12.7 ± 1.1	13.6 ± 1.8	22.3 ± 1.2	17.1 ± 2.8
Sea-nine 211 (10 µM)	70.4 ± 2.5	76.3 ± 4.6	81.1 ± 3.2	83.1 ± 2.5	69.7 ± 4.0

^a The inhibition rate: >60% was intense, 40–60% was media, 20–40% is low, and <20% was no activity, <10% was not shown.

2.2. Identification of the Bioactive Fungi

The three most active fungi were identified by comparing their ITS-rDNA sequences with those in the National Center for Biotechnology Information (NCBI) database, combined with their morphological characteristics. Concretely, the fungus HSXSD-11-1 was identified as *Chrysosporium* sp. whose 647 bp ITS sequence had 99.52% identity to that of *Chrysosporium* sp. 2 JC-2013 (HG329729.1) with the query coverage of 95%. The fungus HSXSD-12 was identified as *Cladosporium* sp. whose 510 bp ITS sequence had 100% identity and 97% query coverage to that of *Cladosporium* sp. CLAD127 (MK111582.1). The fungus CH-6 was identified as *Acrostalagmus luteoalbus* whose 574 bp ITS sequence had 100% identity to that of *A. luteoalbus* J23B1 (MK389477.1) with the query coverage of 95%. The ITS-rDNA sequences of HSXSD-11-1, HSXSD-12, and CH-6 were submitted to GenBank and obtained the accession numbers of MT367260.1, MT367261.1, and MT367202.1, respectively.

2.3. Secondary Metabolites Profile Visualization and Annotation by Molecular Networking

The crude extracts of *A. luteoalbus* CH-6 were subjected to UHPLC-MS/MS analysis to obtain MS² data and then the data were converted into .mzXML format to submit into Global Natural Product Social Molecular Networking (GNPS) online workflow for the molecular network of the fungus secondary metabolites profile (Figure 1). The network was visualized by Cytoscape 3.8.0. The molecular network of the fungus secondary metabolites profile contained 615 nodes and 738 edges, suggesting that 615 compounds with different molecular weights were found in the crude extracts of *A. luteoalbus* CH-6. The 21 yellow nodes were compounds characterized by molecular networking (Table S1). The red nodes were unannotated compounds that might be new compounds according to the result of the molecular networking.

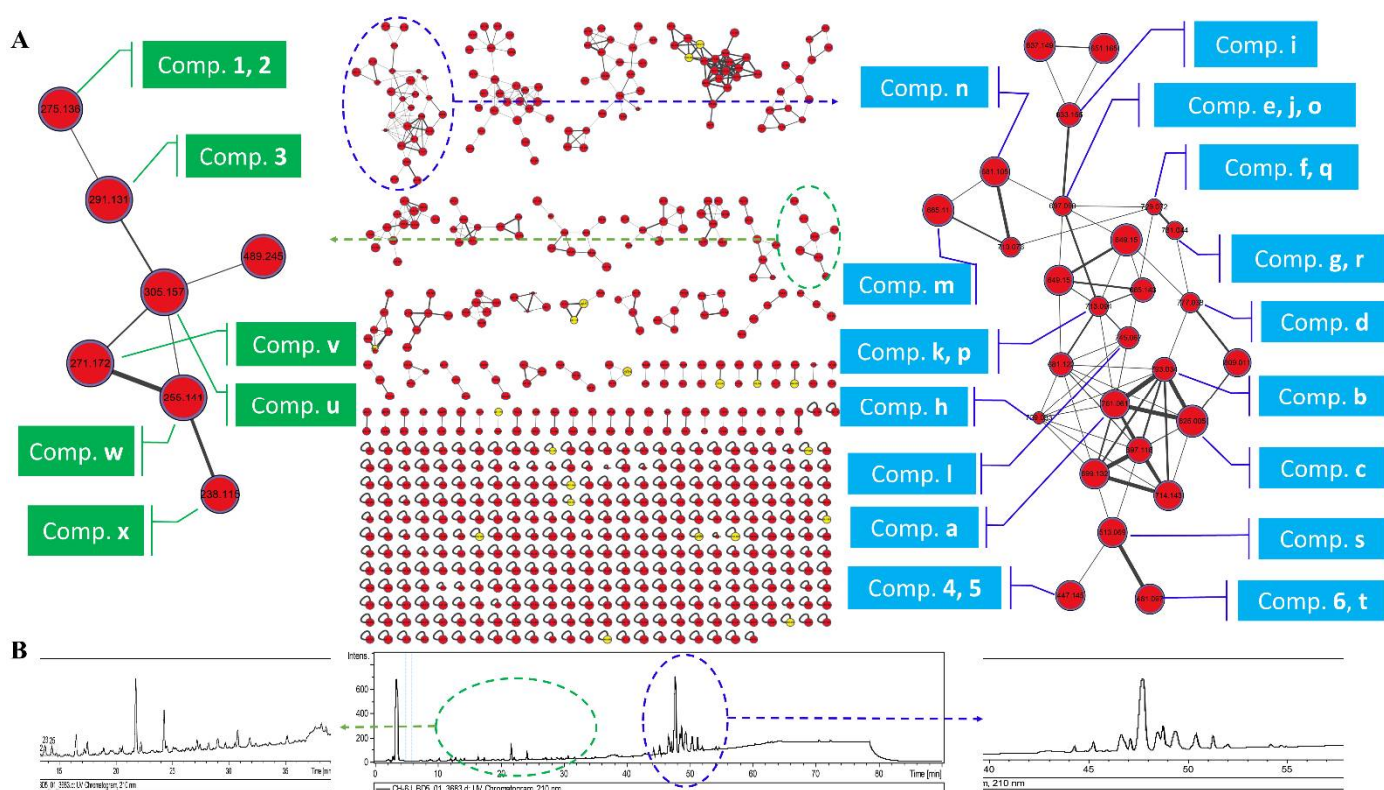
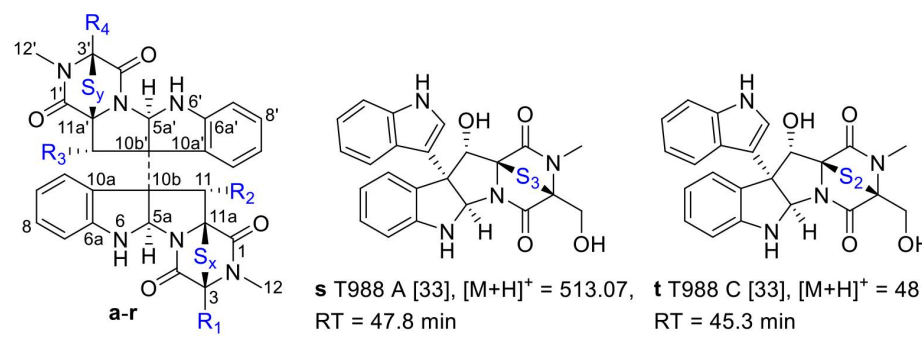


Figure 1. Molecular network of the fungus *A. luteoalbus* CH-6. (A) A full scan of the secondary metabolites' profiles molecular network of the fungus *A. luteoalbus* CH-6 and annotated compounds. (B) HPLC fingerprint of the secondary metabolites of the fungus *A. luteoalbus* CH-6.

In order to identify the compounds' structures in the first family with the maximum nodes, the literature [13–22] about secondary metabolites of *A. luteoalbus* were studied and it was found that thiodiketopiperazine derivatives were the main products of this species, and then annotated 20 analogs in the first family in the molecular network according to the previous studies about thiodiketopiperazine derivatives (Figures 1 and 2) [16,20,26–33].



s T988 A [33], $[M+H]^+ = 513.07$, RT = 47.8 min

t T988 C [33], $[M+H]^+ = 481.10$, RT = 45.3 min

Compounds	R ₁	R ₂	R ₃	R ₄	x	y	Parent MS ([M+H] ⁺)	RT (min)
a Chetracin B [26]	CH ₂ OH	OH	OH	CH ₂ OH	3	2	761.06	46.7
b Chetracin C [26]	CH ₂ OH	OH	OH	CH ₂ OH	3	3	793.03	47.7
c Chetracin F [20]	CH ₂ OH	OH	OH	CH ₂ OH	3	4	825.00	50.6
d Chetracin E [20]	CH ₂ OH	OH	OH	CH ₃	3	3	777.04	49.7
e Chaetocin [27]	CH ₂ OH	H	H	CH ₂ OH	2	2	697.10	50.6
f Chaetocin B [28]	CH ₂ OH	H	H	CH ₂ OH	2	3	729.07	50.5
g Chaetocin C [28]	CH ₂ OH	H	H	CH ₂ OH	3	3	761.04	50.9
h 11 α ,11' α - Dihydroxychaetocin [29]	CH ₂ OH	OH	OH	CH ₂ OH	2	2	729.09	45.8
i Chaetocin monosulfide [27]	CH ₂ OH	H	H	CH ₂ OH	1	1	633.15	42.7
j Verticillin A [30]	CH ₃	OH	OH	CH ₃	2	2	697.10	50.6
k Verticillin B [30]	CH ₂ OH	OH	OH	CH ₃	2	2	713.09	49.0
l Verticillin C [30]	CH ₂ OH	OH	OH	CH ₃	3	2	745.06	48.9
m 11,11'- Dideoxyverticillin A [31]	CH ₃	H	H	CH ₃	2	2	665.11	50.0
n 11'-Deoxyverticillin A [31]	CH ₃	OH	H	CH ₃	2	2	681.12	45.0
o Melinacidin II [16]	CH ₂ OH	H	OH	CH ₃	2	2	697.10	50.6
p Melinacidin III [16]	CH ₂ OH	H	OH	CH ₂ OH	2	2	713.09	49.0
q Gliocladine A [32]	CH ₃	OH	OH	CH ₃	2	3	729.07	50.5
r Gliocladine B [32]	CH ₃	OH	OH	CH ₃	2	4	761.04	50.9

Figure 2. Structures of thiodiketopiperazine derivatives **a–t** and their retention time in HPLC [16,20,26–33].

The α -pyrone derivatives (Figures 1 and 3) were also annotated in the molecular network according to the literature [34–37]. The retention time of the mapped α -pyrones in HPLC fingerprint was pointed out with low yield suggesting that it is difficult to isolate α -pyrone derivatives in the extracts of the fungus *A. luteocalbus* CH-6.

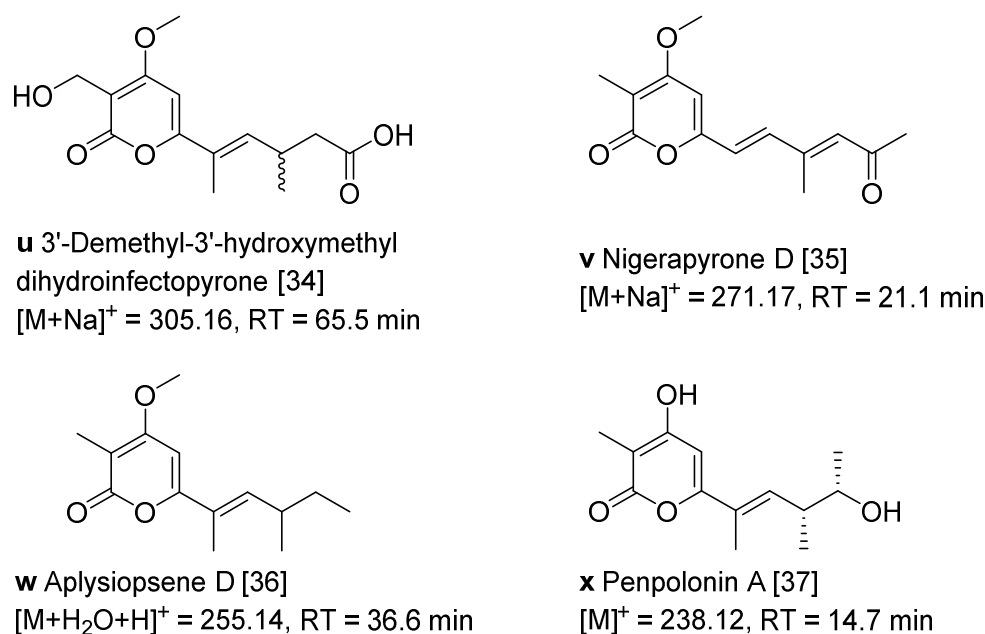


Figure 3. Structures of α -pyrone derivatives **u**–**x** and their retention time in HPLC [34–37].

2.4. Structure Elucidations of Isolated Compounds 1–6

The crude extracts obtained by static culture of *A. luteoalbus* CH-6 showed the strongest antifungal and antibacterial activities. Therefore, they were separated through a bioactivity-guided strategy which led to the isolation of compounds 1–6. Acrostalapyrone A (**1**) (Figure 4) was obtained as an amorphous powder. Its molecular formula, $C_{14}H_{20}O_4$, was determined by HR-ESI-MS spectrum (Figure S9), indicating five degrees of unsaturation. Careful analysis of 1H NMR, ^{13}C NMR, and HSQC spectra (Figures S3–S5) of **1** revealed five methyl signals, including one oxygenated methyl at δ_H 3.91 (3H, s), δ_C 56.3, four methines, including two unsaturated methines at δ_H 6.46 (1H, dd, 10.3, 1.5 Hz), δ_C 136.8 and δ_H 6.13 (1H, s), δ_C 92.4, and one oxygenated methine at δ_H 3.72 (1H, p, 6.4 Hz), δ_C 71.9, and five unsaturated quaternary carbons, including one ester group at δ_C 165.2 (Table 4). The five unsaturated quaternary carbons and two unsaturated methines represented four degrees of unsaturation, combined with the whole five degrees of unsaturation, provided the existence of a ring. All of these NMR spectra characters revealed that **1** was a pyrone compound. Further analyzing these data discovered that **1** was very similar to phomenin A [38] and phomapyrone E [39]. The most obvious differences in the NMR data between **1** and phomenin A were the two olefinic carbons signals in phomenin A were substituted by two methines at δ_H 3.72 (1H, p, 6.4 Hz), δ_C 71.9, and δ_H 2.60 (1H, dp, 10.3, 6.7 Hz), δ_C 41.1 in **1** (Table 4). This was further elucidated by the HMBC correlations from H-9 Me to C-10 and from H-11 to C-9, and the COSY relationships of H-8/H-9, H-9/H-9 Me, H-9/H-10 and H-10/H-11 (Figure 5). Thus the planar structure of **1** was unambiguously confirmed.

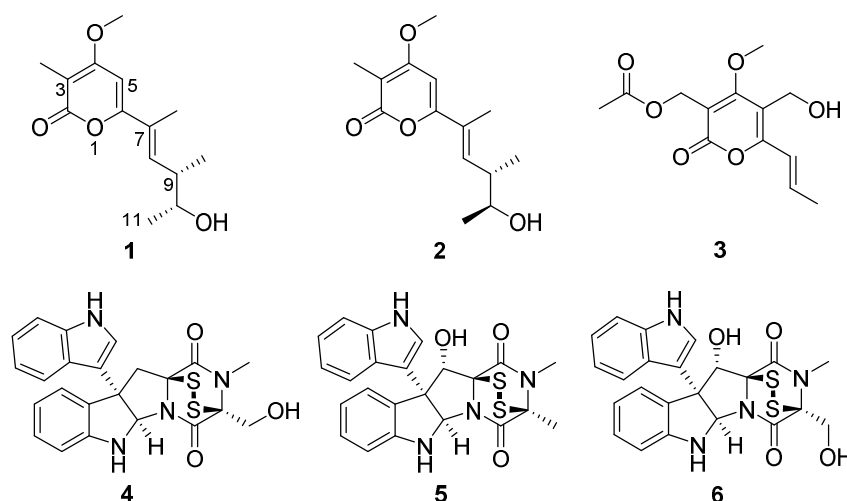


Figure 4. Structures of compounds 1–6.

Table 4. ^1H NMR (600 MHz) and ^{13}C NMR (150 MHz) data of compounds 1 and 2 in CDCl_3 .

No.	1		2	
	δ_{C}	δ_{H}	δ_{C}	δ_{H}
2	165.2, C		165.2, C	
3	102.5, C		102.6, C	
4	166.0, C		166.0, C	
5	92.4, CH	6.13, s	92.5, CH	6.15, s
6	159.8, C		159.7, C	
7	126.4, C		125.7, C	
8	136.8, CH	6.46, dd (10.3, 1.5)	137.0, CH	6.50, dd (10.1, 1.4)
9	41.1, CH	2.60, dp (10.3, 6.7)	41.4, CH	2.57, dp (10.1, 6.8)
10	71.9, CH	3.72, p (6.4)	71.7, CH	3.69, p (6.3)
11	21.3, CH_3	1.17, d (6.4)	20.8, CH_3	1.22, d (6.3)
3-Me	8.8, CH_3	1.94, s	8.8, CH_3	1.938, s
4-OMe	56.3, CH_3	3.91, s	56.3, CH_3	3.91, s
7-Me	13.1, CH_3	1.94, s	13.1, CH_3	1.943, d (1.4)
9-Me	16.5, CH_3	1.09, d (6.7)	16.7, CH_3	1.04, d (6.8)

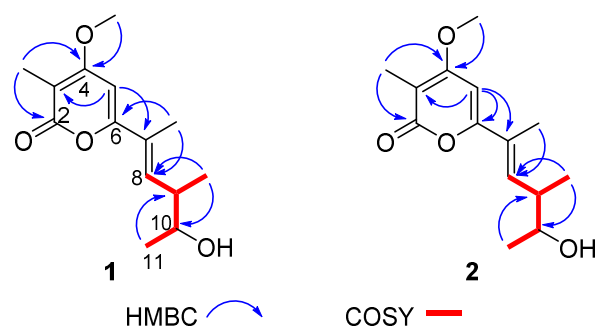


Figure 5. Key COSY and HMBC correlations of compounds 1 and 2.

The relative configurations of **1** were determined by NOESY spectrum (Figure S8). The NOESY correlation between H-7 Me and H-9 revealed the *E* configuration of the olefinic bond at C-7 and C-8 (Figure 6). The cross-peaks of H-8/H-9 Me and H-8/H-11 in the NOESY spectrum proved H-9 Me and H-11 were in the same face. Thus, the relative configurations of **1** were elucidated to be *7E,9S,10R* or *7E,9R,10S*.

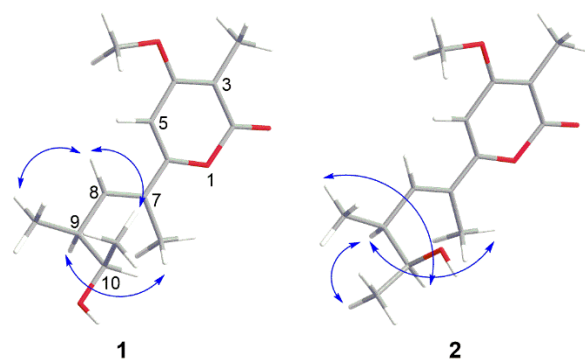


Figure 6. Key NOESY correlations of compounds **1** and **2**.

The absolute configurations of **1** were ascertained by modified Mosher's methods [40,41]. The (*S*)- and (*R*)-MTPA esters of **1**, **1s**, and **1r**, were obtained after treatment of **1** with (*S*)- and (*R*)-MTPA-Cl, respectively. The 10*R* configuration of **1** was revealed by the $\Delta\delta_{\text{H}(1\text{s}-1\text{r})}$ values $\Delta\delta_{\text{H}-11} = +0.07$, $\Delta\delta_{\text{H}-9} = -0.05$, $\Delta\delta_{\text{H}-9 \text{ Me}} = -0.11$, $\Delta\delta_{\text{H}-8} = -0.06$ (Figure 7), following the Mosher's rules. Therefore, the absolute configurations of **1** were confirmed to be 7*E*,9*S*,10*R*. The α -pyrone analogs were named by the name of the isolated fungi and the structural type of the compounds [38,39], compound **1** was named acrostalapyrone A.

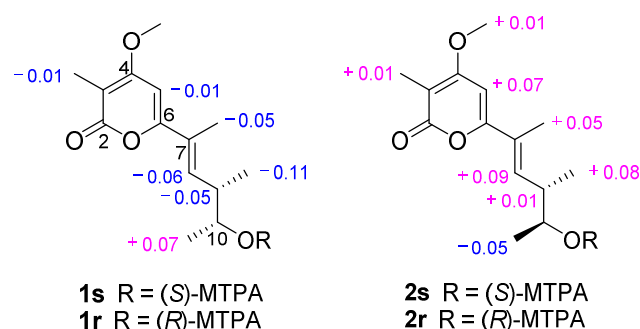


Figure 7. Values of $\Delta\delta_{\text{H}(S-R)}$ (measured in CDCl_3) of the MTPA esters of **1** and **2**.

Acrostalapyrone B (**2**) (Figure 4) was gained as an amorphous powder with the molecular formula of $\text{C}_{14}\text{H}_{20}\text{O}_4$ determined by HR-ESI-MS (Figure S16), which was the same as **1**. The ^1H and ^{13}C NMR data of **2** were very similar to those of **1** (Table 4) indicating that **2** and **1** shared the same plane structure. The obvious differences between the ^{13}C NMR data (Table 4) of **2** and **1** were the higher field shifts of C-7 (δ_{C} 125.7 in **2** vs. δ_{C} 126.4 in **1**) and C-11 (δ_{C} 20.8 in **2** vs. δ_{C} 21.3 in **1**) which might suggest the different configurations of C-7 and C-10 in **2** and **1**.

The relative configurations of **2** were decided by its NOESY spectrum (Figure S15). The cross peak of H-7 Me and H-9 in NOESY proved the *E* configuration of the olefinic bond at C-7 and C-8 (Figure 6) which was the same as **1**. The NOESY relationship of H-9 and H-11 indicated that H-9 and H-11 were on the same side (Figure 6). The NOESY cross-peaks of H-9 Me/H-10 revealed they were on the same side. Thus, the relative configurations of **2** were decided to be 7*E*,9*S*,10*S* or 7*E*,9*R*,10*R*.

The absolute configurations of **2** were confirmed by modified Mosher's methods [40,41]. Compound **2** reacted with (*S*)- and (*R*)-MTPA-Cl, respectively, to obtain (*S*)- and (*R*)-MTPA esters of **2**, **2s**, and **2r**. According to the Mosher's rules, the $\Delta\delta_{\text{H}(2\text{s}-2\text{r})}$ values $\Delta\delta_{\text{H}-11} = -0.05$, $\Delta\delta_{\text{H}-9} = +0.01$, $\Delta\delta_{\text{H}-9 \text{ Me}} = +0.08$, $\Delta\delta_{\text{H}-8} = +0.09$ (Figure 7) confirmed the 10*S* configuration of **2**. Thus, the absolute configurations of **2** were unquestionably ascertained to be 7*E*,9*S*,10*S*, and named acrostalapyrone B.

The optical rotation (OR) values of compounds **1** ($[\alpha]_{\text{D}}^{20} -33$ (*c* 0.067, CH_2Cl_2)) and **2** ($[\alpha]_{\text{D}}^{20} -48$ (*c* 0.067, CH_2Cl_2)) are similar, therefore the absolute configurations of these two compounds cannot be elucidated by OR.

The NMR and OR data of compounds 3–6 (Figures S25–S32, Table S2) were exactly the same as those in the literature [19,32,33,42,43], so 3–6 were elucidated to be multiforisin G [42], luteoalbusin A [19,43], glioclادين C [32], and T988 C [33], respectively.

2.5. Antifungal and Antibacterial Activity Evaluations of Isolated Compounds

All the isolated compounds (1–6) were evaluated for their antifungal and antibacterial activities against one pathomycete *C. albicans*, four pathogenic bacteria *E. coli*, *S. aureus*, *B. subtilis*, *P. aeruginosa*, and ten marine fouling bacteria *P. fulva*, *P. aeruginosa*, *A. salmonicida*, *A. hydrophila*, *V. anguillarum*, *V. harveyi*, *P. halotolerans*, *P. angustum*, *E. cloacae*, and *E. hormaechei*. α -Pyrone 1–3 displayed no obvious antimicrobial activities against all the tested strains, and indole diketopiperazines 4–6 showed antimicrobial activities against a panel of strains (Table 5). Among them, compound 6 exhibited broad-spectrum antimicrobial activities against *C. albicans*, *A. salmonicida*, *P. halotolerans*, *P. fulva*, and *S. aureus* with the MIC values range from 3.125 μ M to 50 μ M (Table 5). Furthermore, compound 6 displayed antibacterial activity two times higher than that of the positive drug Ciprofloxacin against *A. salmonicida*. Compounds 4 and 6 showed significant antimicrobial activities against *C. albicans* and *A. salmonicida* with the MIC values of 3.125–12.5 μ M (Table 5).

Table 5. MIC (μ M) values of compounds 1–6 against a panel of strains.

Strains	<i>C. albicans</i>	<i>A. salmonicida</i>	<i>P. halotolerans</i>	<i>P. fulva</i>	<i>S. aureus</i>
1	>50	>50	>50	>50	>50
2	>50	>50	>50	>50	>50
3	>50	>50	>50	>50	>50
4	12.5	12.5	>50	>50	>50
5	25	50	>50	>50	>50
6	6.25	3.125	25	25	25
CPEX	6.25	6.25	0.195	1.56	3.125

3. Materials and Methods

3.1. General Experimental Procedures

Polymerase chain reaction (PCR) was performed using Thermo T-100 (Thermo Fisher Scientific, Bremen, Germany). Optical rotations were tested on a JASCO P-1020 digital polarimeter (JASCO, Tokyo, Japan). The UV spectrum was recorded using an Implen GmbH NanoPhotometer N50 Touch (Implen, Munich, Germany). NMR spectra were measured on a Bruker AVANCE NEO (Bruker, Switzerland) at 600 MHz for ^1H and 150 MHz for ^{13}C in CDCl_3 . Chemical shifts δ were recorded in ppm, using TMS as the internal standard. HR-MS spectra were measured on a Thermo Scientific LTQ Orbitrap XL spectrometer (Thermo Fisher Scientific, Bremen, Germany). HPLC separation was performed using a Hitachi Primaide Organizer Semi-HPLC system (Hitachi High Technologies, Tokyo, Japan) coupled with a Hitachi Primaide 1430 photodiode array (PDA) detector (Hitachi High Technologies, Tokyo, Japan). A Kromasil C₁₈ semi-preparative HPLC column (250 \times 10 mm, 5 μ m) (Eka Nobel, Bohus, Sweden) was used. Silica gel (200–300 mesh; Qingdao Marine Chemical Group Co., Qingdao, China) and Sephadex LH-20 (Amersham Biosciences Inc., Piscataway, NJ, USA) were used for column chromatography. Thin-layer chromatography was performed on precoated silica gel GF254 plates (Yantai Zifu Chemical Group Co., Yantai, China).

3.2. Isolation and Fermentation of Soil-Derived Fungi from the Fildes Peninsula, Antarctica

The soil samples were collected in ice-free areas (about 10 cm from the surface) of the Fildes Peninsula (S62°12', W58°58') using sterile spatulas and sterilized WhirlPak bags (Sigma-Aldrich, St. Louis, MO, USA), and were transported to the lab in sealed foam package filled with dry ice by airplane, at the Chinese 35th Antarctic expedition in 2019 [44]. The soil samples were incubated in a water bath at 16 °C for 3 min to thaw quickly. In aseptic conditions, 10 g soil sample was mixed thoroughly in 10 mL of sterile distilled

water and stood overnight to obtain a bacterial and fungal suspension. The suspension was diluted into 10^{-1} , 10^{-2} , and 10^{-3} with sterile distilled water, and 100 μL of each dilution along with a stock solution was transferred to PDA culture media and evenly dispersed, respectively, each strength of the suspension was repeated three times to incubate at 4 °C, 16 °C, and 28 °C for one to three weeks until no new colonies appear.

Single colonies of fungi were carefully picked into new PDA culture media repeatedly until only one colony grew in the medium. The purified fungi were transferred into cryogenic vials containing potato dextrose water (PDW) culture media with glycerol protection ($v/v = 3:1$), stored at -80 °C in the State Key Laboratory of Microbial Technology, Institute of Microbial Technology, Shandong University, Qingdao, China. The isolated fungi were selected with different morphological colonies and cultivated in PDW culture media in two Erlenmeyer flasks (300 mL in each 500 mL flask) at 16 °C, one in static (45 days) condition, another one in shock (14 days) condition.

3.3. Extraction and Bioactivities Screening of Fermented Fungi

Each of the fungal fermented culture broth (300 mL) was filtered by two layers of gauze to separate the mycelia from the broth. The mycelia were extracted three times with EtOAc (3×200 mL) and then repeatedly extracted with CH_2Cl_2 -MeOH ($v/v, 1:1$) three times (3×200 mL). The broth was extracted repeatedly with EtOAc (3×300 mL) to get the EtOAc layer. All the extracts were combined and then evaporated to dryness under reduced pressure to afford residues.

The antifungal and antibacterial activities of the fungal extracts were evaluated by the conventional broth dilution assay [45,46]. One pathomycete, *Canidia albicans* (ATCC 10231), four pathogenic bacteria *Escherichia coli* (ATCC 25922), *Staphylococcus aureus* (ATCC 27154), *Bacillus subtilis* (ATCC 6633), *Pseudomonas aeruginosa* (ATCC 27853) were used. Ten marine fouling bacteria *P. fulva*, *P. aeruginosa*, *Aeromonas salmonicida*, *A. hydrophila*, *Vibrio anguillarum*, *V. harveyi*, *Photobacterium halotolerans*, *P. angustum*, *Enterobacter cloacae*, and *E. hormaechei*, isolated from a marine biofilm formed on the bottom of a boat, were also used because microorganisms defending themselves by producing antibiotics against competitive bacteria [47,48]. Cipofloxacin and Sea-nine 211 were used as a positive control, DMSO was used as a negative control.

The bioactive assays were tested in 96 well-plate. Each well contained 198 μL tested strain suspension ($2-5 \times 10^5$ CFU/mL in LB broth) and 2 μL fungal extract (final concentration was 50 $\mu\text{g}/\text{mL}$). Three replicates were performed. The plates were incubated at 37 °C for 24 h, then the OD values were tested at 600 nm in a microplate reader (TriStar² S LB 942 Multimode Reader, Berthold Technologies, Germany). The inhibitory rates were calculated according to the following formula:

$$\text{Inhibition rate (\%)} = (\text{OD}_{\text{DMSO}} - \text{OD}_{\text{extrat}}) / \text{OD}_{\text{DMSO}} \times 100$$

3.4. The Identification of the Bioactive Fungal Strains

The identification of the bioactive fungal strains HSXSD-11-1, HSXSD-12, and CH-6 was conducted by the analysis of the 28S rRNA gene sequences. Each of the fresh fungal mycelium (about 1.00 mg) was dispersed in 50 μL lysis buffer for microorganism to direct PCR (Takara, Cat# 9164), and saved in a metal bath (Yooning, Hangzhou, China) at 100 °C for 30 min to extract its genomic DNA as template DNA. The PCR reactions were performed in a final volume of 50 μL , which was composed of template DNA (3 μL), ITS1 (1 μL), ITS4 (1 μL), PrimeSTAR[®] Max DNA Polymerase (25 μL , Takara, Cat# R045A) and ultrapure water (20 μL), under the following procedures: (1) initial denaturation at 98 °C for 5 min; (2) denaturation at 98 °C for 30 s; (3) annealing at 55 °C for 30 s; (4) extension at 72 °C for 1 min; and (5) final extension at 72 °C for 10 min. Steps (2)–(4) were repeated 30 times. The PCR products were then submitted for sequencing (BGI, China) with the primers ITS1 and ITS4. The sequences of HSXSD-11-1, HSXSD-12, and CH-6 were searched in the NCBI nucleotide collection database through the BLAST program. The three fungi

HSXSD-11-1, HSXSD-12, and CH-6 were identified by the BLAST results, combining with their morphological characteristics.

3.5. Molecular Networking

3.5.1. UHPLC Parameters

Liquid chromatography performed at 30 °C was operated using an HPLC C₁₈ column (Hitachi, 250 mm × 4.6 mm, 5 µm). The PDA detection was recorded from 190 to 400 nm and set wavelengths at 210 and 254 nm for peak characterization. The eluted mobile phases were MeOH (A pump) and H₂O (B pump) with the gradient program (time (min), %A): (0.00, 5); (5.00, 5); (60.00, 100); (75.00, 100); (80.00, 5); and (90.00, 5). The mobile phases flow rate was 1.00 mL/min. The fungal extracts dissolved in methanol were kept at 20 °C and stored in an autosampler and the sample injection volume was 20 µL.

3.5.2. MS² Parameters

MS² analyses were performed using high-resolution Q-TOF mass spectrometry (Bruker impactHD) coupled with an ESI source with the parameters as followed: positive-ion mode, capillary source voltage at 3500 V, drying-gas flow rate at 4 L/min, drying-gas temperature at 200 °C, and end plate offset voltage at 500 V. MS full scan mode was operated from *m/z* 50–1500 (100 ms scan time) with a resolution of 40,000 at *m/z* 1222.

3.5.3. Molecular Network Analysis

The molecular network was created using the online workflow (<https://ccms-ucsd.github.io/GNPSDocumentation/>, accessed on 2 July 2020) on the GNPS website (<http://gnps.ucsd.edu>, accessed on 19 April 2022) [49]. The set parameters of the molecular networking were detailed and described previously [12]. The results were visualized by Cytoscape 3.8.0.

3.6. Extraction and Isolation of Compounds 1–6 from *Acrostalagmus luteoalbus* CH-6

The fungal strain *Acrostalagmus luteoalbus* CH-6 was fermented in a rice culture medium in 200 Erlenmeyer flasks (250 g rice and 350 mL water in each 1000 mL flask) at 16 °C in an air-conditioned room for 60 days. Rice culture medium was used for its eutrophy, simple preparation, low cost, convenience, and ease to obtain. On the other hand, the crude extracts of fungus *A. luteoalbus* CH-6 cultured in rice medium exhibited stronger antimicrobial activities against *C. albicans* and *A. salmonicida*. The fermented culture of *A. luteoalbus* CH-6 (50 kg) was extracted three times with EtOAc (3 × 4000 mL) and then repeatedly extracted with CH₂Cl₂–MeOH (*v/v*, 1:1) three times (3 × 4000 mL). All the extracts were combined and then evaporated to dryness under reduced pressure to afford a residue (376 g). The residue was subjected to vacuum liquid chromatography (VLC) on silica gel using step gradient elution with EtOAc–petroleum ether (PE) (0–100%) and then with MeOH–EtOAc (0–100%) to afford eight fractions (Fr.1–Fr.8). All the eight fractions (Fr.1–Fr.8) were evaluated for their antimicrobial activities against *C. albicans* and *A. salmonicida* and the results showed that the primary bioactive compounds produced by the fungus *A. luteoalbus* CH-6 were focused on Fr.3 and Fr.4. Through the analysis of HPLC–DAD–UV fingerprints (Figure S33) and antimicrobial activity evaluations of Fr.1–Fr.8 (Table S3), Fr.3, and Fr.4 were combined together into new Fr.3 for their similar HPLC–DAD–UV fingerprints and potent antimicrobial activities. Fr.3 was subjected to silica gel chromatographic column (CC) eluting with EtOAc–PE (0–100%) to give eight fractions (Fr.3.1–Fr.3.8). Among them, Fr.3.5 and Fr.3.6 displayed strong antimicrobial activities (Table S3). Fr.3.5 was isolated by CC on Sephadex LH-20 eluted with CH₂Cl₂–MeOH (*v/v*, 1:1) to afford four fractions (Fr.3.5.1–Fr.3.5.4). The bioactivity test results of Fr.3.5.1–Fr.3.5.4 exhibited Fr.3.5.2 and Fr.3.5.3 with significant antimicrobial activities (Table S3). Fr.3.5.2 was purified by using semi-preparative HPLC on an ODS column (Kromasil C₁₈, 250 × 10 mm, 5 µm, 2 mL/min) eluted with 70% MeOH–H₂O to give compounds **1** (3.8 mg) and **2** (3.9 mg). Fr.3.5.3 was first subjected to Sephadex LH-20 CC and further purified by HPLC eluting

with 80% MeOH–H₂O to gain **4** (7.8 mg) and **5** (29.2 mg). Fr.3.6 was separated on Sephadex LH-20 CC eluted with CH₂Cl₂–MeOH (v/v, 1:1) to afford four fractions (Fr.3.6.1–Fr.3.6.4). Fr.3.6.1 showed obvious antimicrobial activities (Table S3) and was further purified by HPLC eluted with 65% MeOH–H₂O to give compounds **3** (4.1 mg) and **6** (10.9 mg).

Acrostalapyrone A (**1**): amorphous powder; $[\alpha]_D^{20} -33$ (c 0.067, CH₂Cl₂); UV (CH₂Cl₂) λ_{\max} (log ϵ) 236 (4.86), 332 (4.74) nm; ¹H and ¹³C NMR data, see Table 4; HR-ESI-MS m/z 253.1432 [M + H]⁺ (calcd. for C₁₄H₂₁O₄, 253.1434), 275.1250 [M + Na]⁺ (calcd. for C₁₄H₂₀O₄Na, 275.1254).

Acrostalapyrone B (**2**): amorphous powder; $[\alpha]_D^{20} -48$ (c 0.067, CH₂Cl₂); UV (CH₂Cl₂) λ_{\max} (log ϵ) 234 (4.67), 333 (4.48) nm; ¹H and ¹³C NMR data, see Table 4; HR-ESI-MS m/z 253.1434 [M + H]⁺ (calcd. for C₁₄H₂₁O₄, 253.1434), 275.1252 [M + Na]⁺ (calcd. for C₁₄H₂₀O₄Na, 275.1254).

3.7. Preparation of the (S)- and (R)-MTPA Esters of **1** and **2**

(S)-(–)- α -methoxy- α -(trifluoromethyl)phenylacetyl chloride ((S)-MTPA-Cl) (10 μ L) was added to a stirred pyridine solution (500 μ L) of **1** (1.0 mg) and 4-(dimethylamino)pyridine (2.0 mg). The mixture was stirred at rt for 10 h. The reaction mixture was evaporated to dryness under reduced pressure to get the reaction product, and then purified by HPLC eluted with 80% MeOH–H₂O to give (S)-MTPA ester **1s**. Treatment of **1** (1.0 mg) with (R)-MTPA-Cl (10 μ L) as described above yielded the corresponding (R)-MTPA ester **1r**. By the same procedure as for the preparation of the (S)- and (R)-MTPA esters of **1**, (S)-MTPA ester (**2s**) and (R)-MTPA ester (**2r**) of **2** were obtained.

(S)-MTPA ester of **1** (**1s**): ¹H NMR (600 MHz, CDCl₃) δ 7.53 (dd, $J = 6.8, 2.9$ Hz, 2H, aromatic protons), 7.43–7.37 (m, 3H, aromatic protons), 6.34 (dd, $J = 10.2, 1.4$ Hz, 1H, H-8), 6.11 (s, 1H, H-5), 5.10–5.05 (m, 1H, H-10), 3.90 (s, 3H, 4-OMe), 3.57 (d, $J = 1.3$ Hz, 3H, OMe-MTPA), 2.79 (dq, $J = 10.2, 6.8$ Hz, 1H, H-9), 1.94 (s, 3H, 3-Me), 1.84 (d, $J = 1.4$ Hz, 3H, 7-Me), 1.32 (d, $J = 6.3$ Hz, 3H, H-11), 0.95 (d, $J = 6.8$ Hz, 3H, 9-Me); HR-APCI-MS m/z 469.1828 [M + H]⁺ (calcd. for C₂₄H₂₆O₆F₃, 469.1833).

(R)-MTPA ester of **1** (**1r**): ¹H NMR (600 MHz, CDCl₃) δ 7.52 (dd, $J = 6.8, 3.0$ Hz, 2H, aromatic protons), 7.44–7.38 (m, 3H, aromatic protons), 6.40 (dd, $J = 10.2, 1.4$ Hz, 1H, H-8), 6.12 (s, 1H, H-5), 5.08–5.04 (m, 1H, H-10), 3.90 (s, 3H, 4-OMe), 3.52 (d, $J = 1.2$ Hz, 3H, OMe-MTPA), 2.84 (dq, $J = 10.2, 6.7$ Hz, 1H, H-9), 1.95 (s, 3H, 3-Me), 1.89 (d, $J = 1.4$ Hz, 3H, 7-Me), 1.25 (d, $J = 6.3$ Hz, 3H, H-11), 1.06 (d, $J = 6.7$ Hz, 3H, 9-Me); HR-APCI-MS m/z 469.1826 [M + H]⁺ (calcd. for C₂₄H₂₆O₆F₃, 469.1833).

$\delta_{1s}-\delta_{1r}$: H-8 = –0.06, H-5 = –0.01, H-10 = +0.02, H-9 = –0.05, H-3Me = –0.01, H-7Me = –0.05, H-11 = +0.07, H-9Me = –0.11.

(S)-MTPA ester of **2** (**2s**): ¹H NMR (600 MHz, CDCl₃) δ 7.49–7.44 (m, 2H, aromatic protons), 7.37–7.30 (m, 3H, aromatic protons), 6.36 (dd, $J = 10.0, 1.4$ Hz, 1H, H-8), 6.09 (s, 1H, H-5), 5.03 (p, $J = 6.4$ Hz, 1H, H-10), 3.89 (s, 3H, 4-OMe), 3.47 (d, $J = 1.2$ Hz, 3H, OMe-MTPA), 2.85 (dq, $J = 10.0, 6.8$ Hz, 1H, H-9), 1.96 (s, 3H, 3-Me), 1.86 (d, $J = 1.4$ Hz, 3H, 7-Me), 1.30 (d, $J = 6.4$ Hz, 3H, H-11), 1.07 (d, $J = 6.8$ Hz, 3H, 9-Me); HR-APCI-MS m/z 469.1828 [M + H]⁺ (calcd. for C₂₄H₂₆O₆F₃, 469.1833).

(R)-MTPA ester of **2** (**2r**): ¹H NMR (600 MHz, CDCl₃) δ 7.48 (dd, $J = 6.7, 2.9$ Hz, 2H, aromatic protons), 7.35–7.30 (m, 3H, aromatic protons), 6.27 (dd, $J = 9.9, 1.4$ Hz, 1H, H-8), 6.02 (s, 1H, H-5), 5.04 (p, $J = 6.4$ Hz, 1H, H-10), 3.88 (s, 3H, 4-OMe), 3.56 (d, $J = 1.3$ Hz, 3H, OMe-MTPA), 2.84 (dq, $J = 9.9, 6.8$ Hz, 1H, H-9), 1.95 (s, 3H, 3-Me), 1.81 (d, $J = 1.4$ Hz, 3H, 7-Me), 1.35 (d, $J = 6.4$ Hz, 3H, H-11), 0.99 (d, $J = 6.8$ Hz, 3H, 9-Me); HR-APCI-MS m/z 469.1830 [M + H]⁺ (calcd. for C₂₄H₂₆O₆F₃, 469.1833).

$\delta_{2s}-\delta_{2r}$: H-8 = +0.09, H-5 = +0.07, H-10 = –0.01, 4-OMe = +0.01, H-9 = +0.01, H-3Me = +0.01, H-7Me = +0.05, H-11 = –0.05, H-9Me = +0.08.

3.8. Antibacterial and Antifungal Activity Evaluations of the Isolated Compounds **1–6**

The preliminary screening method of antibacterial and antifungal activities of **1–6** was the same as those of fungal extracts. The MIC values of some active target compounds were

evaluated using the 2-fold serial-dilution method. The concentrations of the compounds ranged from 100 μM to 0.78125 μM . The other steps were the same as the method of primary screening.

4. Conclusions

In summary, three antimicrobial fungi, *Chrysosporium* sp. HSXSD-11-1, *Cladosporium* sp. HSXSD-12, and *Acrostalagmus luteoalbus* CH-6, were discovered from the soil samples of the Fildes Peninsula, Antarctica. Bioassay-guided searching of antimicrobial secondary metabolites of *A. luteoalbus* CH-6, combined with molecular networking, led to the isolation of two new α -pyrones, acrostalapyrones A (1) and B (2), and one known analog, multiforisin G (3), as well as three known indole diketopiperazines, luteoalbusin A (4), glioclidine C (5), and T988 C (6). Compounds 4 and 6 showed significant antimicrobial activities against *C. albicans* and *A. salmonicida*. In particular, the antibacterial activity against *A. salmonicida* of 6 displayed two times higher than that of the positive drug Ciprofloxacin. This is the first time to find α -pyrones in the fungal genus *Acrostalagmus* and the first report to discover significant antimicrobial activities of compounds 4 and 6 against *C. albicans* and *A. salmonicida*. This study further demonstrates the great potential of Antarctic fungi in the development of new compounds and antibiotics.

Supplementary Materials: The following supporting information can be downloaded at: <https://www.mdpi.com/article/10.3390/md20050334/s1>, Figure S1: Fermented cultivable fungal colonies from the Fildes Peninsula, Antarctica; Figure S2: The colony morphology (left) and light microscopy (right) of *A. luteoalbus* CH-6; Figures S3–S32: NMR and MS data of compounds 1–6, 1s, 1r, 2s, and 2r; Figure S33: HPLC fingerprints of separated fractions Fr.1–Fr.8 of *A. luteoalbus* CH-6. Table S1: Identified compounds by molecular networking; Table S2: OR values of compounds 4–6; Table S3: Antimicrobial activities of the separated fractions (50 $\mu\text{g}/\text{mL}$) of *A. luteoalbus* CH-6.

Author Contributions: Conceptualization, T.S.; methodology, T.S., X.-Q.L. and Z.-M.W.; software, T.S.; validation, Y.-Y.Y., J.-J.D. and D.-Y.S.; formal analysis, T.S.; investigation, T.S., X.-Q.L. and Z.-M.W.; resources, L.Z.; data curation, T.S. and D.-Y.S.; writing—original draft preparation, T.S.; writing—review and editing, D.-Y.S.; visualization, X.-Q.L.; supervision, D.-Y.S.; project administration, D.-Y.S.; funding acquisition, T.S., X.-Q.L., J.-J.D. and D.-Y.S. All authors have read and agreed to the published version of the manuscript.

Funding: This work was supported by the National Natural Science Foundation of China (No. 82104029; 82003787); the Shandong Provincial Natural Science Foundation (No. ZR2020QD111; ZR2020QH364); the Top-notch Young Professionals; the Fund of Taishan Scholar Project; the Qingdao Science and Technology Benefit People Demonstration Guide Special Project (20-3-4-20-nsh) and the Fundamental Research Funds of Shandong University (2020GN033).

Institutional Review Board Statement: Not applicable.

Informed Consent Statement: Not applicable.

Data Availability Statement: The datasets presented in this study can be found in online repositories. The names of the repository/repositories and accession number(s) can be found below: <https://www.ncbi.nlm.nih.gov/nuccore/MT367260>, accessed on 21 April 2020; <https://www.ncbi.nlm.nih.gov/nuccore/MT367261>, accessed on 21 April 2020; <https://www.ncbi.nlm.nih.gov/nuccore/MT367202>, accessed on 21 April 2020.

Acknowledgments: We would like to thank the Antarctic Great Wall National Observation and Research Station of Polar Ecosystem for sample collection; Jing-Yao Qu, Jing Zhu, Guan-Nan Lin, and Zhi-Feng Li in MS, Hai-Yan Sui in NMR for help and guidance from the State Key laboratory of Microbial Technology of Shandong University.

Conflicts of Interest: The authors declare that the research was conducted in the absence of any commercial or financial relationships that could be construed as a potential conflict of interest.

References

1. O'Neill, J. *Review on Antimicrobial Resistance. Tackling Drug-Resistant Infections Globally: Final Report and Recommendations*; Wellcome Trust and HM Government: London, UK, 2016.
2. Monowar, T.; Rahman, M.S.; Bhore, S.J.; Sathasivam, K.V. Endophytic bacteria *Enterobacter hormaechei* fabricated silver nanoparticles and their antimicrobial activity. *Pharmaceutics* **2021**, *13*, 511. [[CrossRef](#)] [[PubMed](#)]
3. Lomazzi, M.; Moore, M.; Johnson, A.; Balasegaram, M.; Borisch, B. Antimicrobial resistance—moving forward? *BMC Public Health* **2019**, *19*, 858–863. [[CrossRef](#)] [[PubMed](#)]
4. WHO. *Global Antimicrobial Resistance and Use Surveillance System (GLASS) Report 2021*; World Health Organization: Geneva, Switzerland, 2021; License: CC BY-NC-SA 3.0 IGO.
5. CDC. *Antibiotic Resistance Threats in the United States*; Department of Health and Human Services: Atlanta, GA, USA, 2019.
6. WHO. *2019 Antibacterial Agents in Clinical Development: An Analysis of the Antibacterial Clinical Development Pipeline*; World Health Organization: Geneva, Switzerland, 2019; License: CC BY-NC-SA 3.0 IGO.
7. Butler, M.S.; Buss, A.D. Natural products—the future scaffolds for novel antibiotics? *Biochem. Pharmacol.* **2006**, *71*, 919–929. [[CrossRef](#)] [[PubMed](#)]
8. Genilloud, O. Current challenges in the discovery of novel antibacterials from microbial natural products. *Recent Pat. Anti-Infect. Drug Discov.* **2012**, *7*, 189–204. [[CrossRef](#)] [[PubMed](#)]
9. Cong, B.; Yin, X.; Deng, A.; Shen, J.; Tian, Y.; Wang, S.; Yang, H. Diversity of cultivable microbes from soil of the Fildes Peninsula, Antarctica, and their potential application. *Front. Microbiol.* **2020**, *11*, 570836. [[CrossRef](#)] [[PubMed](#)]
10. Shah, M.; Sun, C.; Zhang, G.; Che, Q.; Li, D. Antibacterial polyketides from Antarctica sponge-derived fungus *Penicillium* sp. HDN151272. *Mar. Drugs* **2020**, *18*, 71. [[CrossRef](#)]
11. Sun, C.; Zhang, Z.; Ren, Z.; Yu, L.; Zhu, T. Antibacterial cyclic tripeptides from Antarctica-sponge-derived fungus *Aspergillus insulicola* HDN151418. *Mar. Drugs* **2020**, *18*, 532. [[CrossRef](#)]
12. Shi, T.; Yu, Y.-Y.; Dai, J.-J.; Zhang, Y.-T.; Hu, W.-P.; Zheng, L.; Shi, D.-Y. New polyketides from the Antarctic fungus *Pseudogymnoascus* sp. HSX2#-11. *Mar. Drugs* **2021**, *19*, 168.
13. Ellestad, G.A.; Evans, R.H., Jr.; Kunstmann, M.P. Structure of a C¹⁷ antifungal terpenoid from an unidentified *Acrostalagmus* species. *J. Amer. Chem. Soc.* **1969**, *91*, 2134–2136. [[CrossRef](#)]
14. Ellestad, G.A.; Evans, R.H., Jr.; Kunstmann, M.P.; Lancaster, J.E.; Morton, G.O. Structure and chemistry of antibiotic LL-Z1271 α , an antifungal carbon-17 terpene. *J. Amer. Chem. Soc.* **1970**, *92*, 5483–5489. [[CrossRef](#)]
15. Argoudelis, A.D.; Reusser, F. Melinacidins, a new family of antibiotics. *J. Antibiot.* **1971**, *24*, 383–389. [[CrossRef](#)] [[PubMed](#)]
16. Argoudelis, A.D. Melinacidins II, III, and IV. New 3,6-epidithiadiketopiperazine antibiotics. *J. Antibiot.* **1972**, *25*, 171–178. [[CrossRef](#)] [[PubMed](#)]
17. Sato, M.; Kakisawa, H. Structures of three new C¹⁶ terpenoids from an *Acrostalagmus* fungus. *J. Chem. Soc. Perkin Trans.* **1976**, *1*, 2407–2413. [[CrossRef](#)]
18. Rojas, N.L.; Voget, C.E.; Hours, R.A.; Cavalitto, S.F. Purification and characterization of a novel alkaline α -L-rhamnosidase produced by *Acrostalagmus luteoalbus*. *J. Ind. Microbiol. Biotechnol.* **2011**, *38*, 1515–1522. [[CrossRef](#)] [[PubMed](#)]
19. Wang, F.-Z.; Huang, Z.; Shi, X.-F.; Chen, Y.-C.; Zhang, W.-M.; Tian, X.-P.; Li, J.; Zhang, S. Cytotoxic indole diketopiperazines from the deep sea-derived fungus *Acrostalagmus luteoalbus* SCSIO F457. *Bioorg. Med. Chem. Lett.* **2012**, *22*, 7265–7267. [[CrossRef](#)] [[PubMed](#)]
20. Yu, G.; Wang, Y.; Yu, R.; Feng, Y.; Wang, L.; Che, Q.; Gu, Q.; Li, D.; Li, J.; Zhu, T. Chetracins E and F, cytotoxic epipolythiodioxopiperazines from the marine-derived fungus *Acrostalagmus luteoalbus* HDN13-530. *RSC Adv.* **2018**, *8*, 53–58. [[CrossRef](#)]
21. Cao, J.; Li, X.-M.; Meng, L.-H.; Konuklugil, B.; Li, X.; Li, H.-L.; Wang, B.-G. Isolation and characterization of three pairs of indolediketopiperazine enantiomers containing infrequent *N*-methoxy substitution from the marine algal-derived endophytic fungus *Acrostalagmus luteoalbus* TK-43. *Bioorg. Chem.* **2019**, *90*, 103030. [[CrossRef](#)]
22. Cao, J.; Li, X.-M.; Li, X.; Li, H.-L.; Konuklugil, B.; Wang, B.-G. Uncommon *N*-methoxyindolediketopiperazines from *Acrostalagmus luteoalbus*, a marine algal isolate of endophytic fungus. *Chin. J. Chem.* **2021**, *39*, 2808–2814. [[CrossRef](#)]
23. Ramos, A.E.F.; Evanno, L.; Poupon, E.; Champy, P.; Beniddir, M.A. Natural products targeting strategies involving molecular networking: Different manners, one goal. *Nat. Prod. Rep.* **2019**, *36*, 960–980. [[CrossRef](#)]
24. Nothias, L.-F.; Petras, D.; Schmid, R.; Dührkop, K.; Rainer, J.; Sarvepalli, A.; Protsyuk, I.; Ernst, M.; Tsugawa, H.; Fleischauer, M. Feature-based molecular networking in the GNPS analysis environment. *Nat. Methods* **2020**, *17*, 905–908. [[CrossRef](#)]
25. Hou, X.M.; Li, Y.Y.; Shi, Y.W.; Fang, Y.W.; Shao, C.L. Integrating molecular networking and ¹H NMR to target the isolation of chrysogeamides from a library of marine-derived *Penicillium* fungi. *J. Org. Chem.* **2019**, *84*, 1228–1237. [[CrossRef](#)] [[PubMed](#)]
26. Li, L.; Li, D.; Luan, Y.; Gu, Q.; Zhu, T. Cytotoxic metabolites from the Antarctic psychrophilic fungus *Oidiodendron truncatum*. *J. Nat. Prod.* **2012**, *75*, 920–927. [[CrossRef](#)] [[PubMed](#)]
27. Cherblanc, F.; Lo, Y.-P.; De Gussem, E.; Alcazar-Fuoli, L.; Bignell, E.; He, Y.; Chapman-Rothe, N.; Bultinck, P.; Herrebout, W.A.; Brown, R.; et al. On the determination of the stereochemistry of semisynthetic natural product analogues using chiroptical spectroscopy: Desulfurization of epidithiodioxopiperazine fungal metabolites. *Chem. Eur. J.* **2011**, *17*, 11868–11875. [[CrossRef](#)] [[PubMed](#)]
28. Saito, T.; Suzuki, Y.; Koyama, K.; Natori, S.; Iitaka, Y.; Kinoshita, T. Chetracin A and chaetocins B and C, three new epipolythiodioxopiperazines from *Chaetomium* spp. *Chem. Pharm. Bull.* **1988**, *36*, 1942–1956. [[CrossRef](#)]

29. Saito, T.; Koyama, K.; Natori, S.; Iitaka, Y. Chetracin A, a new epipolythiodioxopiperazine having a tetrasulfide bridge from *Chaetomium abuense* and *C. retardatum*. *Tetrahedron Lett.* **1985**, *26*, 4731–4734. [[CrossRef](#)]
30. Minato, H.; Matsumoto, M.; Katayama, T. Studies on the metabolites of *Verticillium* sp. Structures of verticillins A, B, and C. *J. Chem. Soc. Perkin. Trans.* **1973**, *1*, 1819–1825. [[CrossRef](#)]
31. Byeng, W.S.; Jensen, P.R.; Kauffman, C.A.; Fenical, W. New cytotoxic epidthiodioxopiperazines related to verticillin A from a marine isolate of the fungus *Penicillium*. *Nat. Prod. Lett.* **1999**, *13*, 213–222.
32. Dong, J.-Y.; He, H.-P.; Shen, Y.-M.; Zhang, K.-Q. Nematicidal epipolysulfanyldioxopiperazines from *Gliocladium roseum*. *J. Nat. Prod.* **2005**, *68*, 1510–1513. [[CrossRef](#)]
33. Feng, Y.; Blunt, J.W.; Cole, A.L.; Munro, M.H. Novel cytotoxic thiodiketopiperazine derivatives from a *Tilachlidium* sp. *J. Nat. Prod.* **2004**, *67*, 2090–2092. [[CrossRef](#)]
34. Proksch, P.; Ebel, R.; Edrada, R.; Riebe, F.; Liu, H.; Diesel, A.; Bayer, M.; Li, X.; Lin, W.H.; Grebenyuk, V.; et al. Sponge-associated fungi and their bioactive compounds: The *Suberites* case. *Bot. Mar.* **2008**, *51*, 209–218. [[CrossRef](#)]
35. Liu, D.; Li, X.-M.; Meng, L.; Li, C.-S.; Gao, S.-S.; Shang, Z.; Proksch, P.; Huang, C.-G.; Wang, B.-G. Nigerapyrones A–H, α -pyrone derivatives from the marine mangrove-derived endophytic fungus *Aspergillus niger* MA-132. *J. Nat. Prod.* **2011**, *74*, 1787–1791. [[CrossRef](#)] [[PubMed](#)]
36. Rukachaisirikul, V.; Khamthong, N.; Sukpondma, Y.; Phongpaichit, S.; Hutadilok-Towatana, N.; Graidist, P.; Sakayaroj, J.; Kirtikara, K. Cyclohexene, diketopiperazine, lactone and phenol derivatives from the sea fan-derived fungi *Nigrospora* sp. PSU-F11 and PSU-F12. *Arch. Pharmacol. Res.* **2010**, *33*, 375–380. [[CrossRef](#)] [[PubMed](#)]
37. Ma, Y.; Wen, Y.; Cheng, H.; Deng, J.; Peng, Y.; Bahetejiang, Y.; Huang, H.; Wu, C.; Yang, X.; Pang, K. Penpolonin A–E, cytotoxic α -pyrone derivatives from *Penicillium polonicum*. *Bioorg. Med. Chem. Lett.* **2021**, *40*, 127921. [[CrossRef](#)] [[PubMed](#)]
38. Tringali, C.; Parisi, A.; Piattelli, M.; Magnano Di San Lio, G. Phomenins A and B, bioactive polypropionate pyrones from culture fluids of *Phoma tracheiphila*. *Nat. Prod. Lett.* **1993**, *3*, 101–106. [[CrossRef](#)]
39. Pedras, M.S.C.; Chumala, P.B. Phomapyrones from blackleg causing phytopathogenic fungi: Isolation, structure determination, biosyntheses and biological activity. *Phytochemistry* **2005**, *66*, 81–87. [[CrossRef](#)]
40. Kusumi, T.; Ohtani, I.; Inouye, Y.; Kakisawa, H. Absolute configurations of cytotoxic marine cembranolides; consideration of Mosher's method. *Tetrahedron Lett.* **1988**, *29*, 4731–4734. [[CrossRef](#)]
41. Li, F.; Ye, Z.; Huang, Z.; Chen, X.; Sun, W.; Gao, W.; Zhang, S.; Cao, F.; Wang, J.; Hu, Z.; et al. New α -pyrone derivatives with herbicidal activity from the endophytic fungus *Alternaria brassicicola*. *Bioorg. Chem.* **2021**, *117*, 105452. [[CrossRef](#)]
42. Fujimoto, H.; Sumino, M.; Nagano, J.; Natori, H.; Okuyama, E.; Yamazaki, M. Immunomodulatory constituents from three ascomycetes, *Gelasinospora heterospora*, *G. multiforis*, and *G. longispora*. *Chem. Pharm. Bull.* **1999**, *47*, 71–76. [[CrossRef](#)]
43. Adams, T.C.; Payette, J.N.; Cheah, J.H.; Movassaghi, M. Concise total synthesis of (+)-luteoalbusins A and B. *Org. Lett.* **2015**, *17*, 4268–4271. [[CrossRef](#)]
44. Shi, T.; Li, X.-Q.; Zheng, L.; Zhang, Y.-T.; Dai, J.-J.; Shang, E.-L.; Yu, Y.-Y.; Zhang, Y.-H.; Hu, W.-P.; Shi, D.-Y. Sesquiterpenoids from the Antarctic fungus *Pseudogymnoascus* sp. H5X2#-11. *Front. Microbiol.* **2021**, *12*, 688202.
45. Appendino, G.; Gibbons, S.; Giana, A.; Pagani, A.; Grassi, G.; Stavri, M.; Smith, E.; Rahman, M.M. Antibacterial cannabinoids from *Cannabis sativa*: A structure-activity study. *J. Nat. Prod.* **2008**, *71*, 1427–1430. [[CrossRef](#)] [[PubMed](#)]
46. Andrews, J.M. Determination of minimum inhibitory concentrations. *J. Antimicrob. Chemother.* **2001**, *48*, 5–16. [[CrossRef](#)]
47. Qian, P.-Y.; Xu, Y.; Fusetani, N. Natural products as antifouling compounds: Recent progress and future perspectives. *Biofouling* **2009**, *26*, 223–234. [[CrossRef](#)] [[PubMed](#)]
48. Kanagasabhathay, M.; Nagata, S. Cross-species induction of antibacterial activity produced by epibiotic bacteria isolated from Indian marine sponge *Pseudoceratina purpurea*. *World J. Microbiol. Biotechnol.* **2008**, *24*, 687–691. [[CrossRef](#)]
49. Wang, M.; Carver, J.J.; Phelan, V.V.; Sanchez, L.M.; Bandeira, N. Sharing and community curation of mass spectrometry data with Global Natural Products Social Molecular Networking. *Nat. Biotechnol.* **2016**, *34*, 828–837. [[CrossRef](#)] [[PubMed](#)]